Inorganica Chimica Acta 394 (2013) 107–116

Contents lists available at SciVerse ScienceDirect

Inorganica Chimica Acta

journal homepage: www.elsevier.com/locate/ica

Imidazole containing palladium(II) complexes as efficient pre-catalyst systems for Heck and Suzuki coupling reaction: Synthesis, structural characterization and catalytic properties

Manoj Trivedi [a,*], Gurmeet Singh [a], R. Nagarajan [a], Nigam P. Rath [b,*]

[a] Department of Chemistry, University of Delhi, Delhi 110007, India
[b] Department of Chemistry & Biochemistry and Centre for Nanoscience, University of Missouri-St. Louis, One University Boulevard, St. Louis, MO 63121-4499, USA

ARTICLE INFO

Article history:
Received 19 March 2012
Received in revised form 7 August 2012
Accepted 7 August 2012
Available online 17 August 2012

Keywords:
Palladium(II) complex
X-ray structure
Cross-coupling reaction
Palladium nanoparticle

ABSTRACT

A series of new palladium(II) complexes of the general formula *trans*-[PdX_2L_2] [X = Cl, Br; L = 1-phenylimidazole (PI), 1-(4-methoxyphenyl)-1*H*-imidazole (MPI), 4(5)-(hydroxymethyl)-imidazole (HMI), 1-(4-cyanophenyl)-imidazole) (CPI)] [X = Cl; L = PI(**1**), X = Cl; L = MPI(**2**), X = Cl; L = HMI(**3**), X = Cl; L = CPI(**4**), X = Br; L = PI(**5**), X = Br; L = MPI(**6**), X = Br; L = HMI(**7**), X = Br; L = CPI(**8**)] have been synthesized. Resulting complexes have been characterized by elemental analyses, IR, ^1H and ^{13}C NMR, FAB-MS and electronic spectral studies. The molecular structures of **1**, and **6** have been determined by single crystal X-ray analyses. The catalytic activities of all the Pd complexes (**1**–**8**) in coupling reactions such as the Mizoroki–Heck and Suzuki–Miyaura coupling reaction have also been studied. Among the **1**–**8** complexes in our investigations, **1**, **2**, **5**, and **6** exhibited highest catalytic activity as compared to **3**, **4**, **7**, and **8** complexes which is due to formation of Pd nanoparticles that might be actually the true active species.

1. Introduction

Remarkable progress has been made in the area of palladium complexes due to their promising properties in applied sciences, mostly owing to high efficiency as homogenous catalysts in a variety of coupling reactions in organic synthesis [1–5]. Currently, well-designed ligands have contributed significantly to improving catalytic activity. The majority of them are phosphine based ligands, because of increasing bulkiness and also introducing electron-donating functions increase the reactivity of aryl halides, enabling their use as substrates [6–8]. There are, however, a number of problems that are frequently encountered in the use of phosphine ligands in catalysis. For example, the degradation of P—C bonds is notorious and can result in deactivation of the catalyst as well as the scrambling of the coupling partners with the phosphine substituents [9,10]. This, in addition to their sensitivity to moisture and aerial oxidation, their high toxicity, often laborious synthesis and loss during product extraction, has driven research into alternatives to phosphines. Furthermore, because of recent development of palladacyclic catalysts [11–19] and *N*-heterocyclic carbene palladium catalysts [20–33] should be mentioned as well. With regard to other types of ligands in coupling reactions, Dai et al. have focused on the development of amide-based phosphines as the P,O-ligands for coupling reactions [34–37]. Čermák et al. have reported diphosphinoazine-Pd(II) complexes that feature a novel tridentate ligand for Mizoroki–Heck reactions with high TON and TOF (h^{-1}) [38,39]. Various attempts have been adopted to improve the Mizoroki–Heck reaction by activating aryl chloride using Pd compounds such as $(CH_3CN)_2$—$PdCl_2$—PPh_4Cl [40], $Pd(OAc)_2$ with excess $P(OEt)_3$ [41] and heterogeneous Pd/C as catalysts [42,43]. In contrast to phosphine-type ligands, the low toxicity and stability of nitrogen-based ligands, such as imidazole derivatives, have attracted the interest of synthetic organic chemists. Togni and Venanzi [44] exhaustively discussed the relevance of N-donors in organometallic chemistry. Although, to date, a large number of N-ligand derivatives have found for practical applications but the search for new, more effective and/or selective species is still in progress. However, there are few reports of highly catalytic reactive complexes bearing nitrogen ligands, although there are many reports of nitrogen ligands [45–61]. We are interested in the possibility of using imidazole derivatives as ligands because they are structurally simple, readily available, and inexpensive, and they allow for simplistic introduction of various substituents into their structure. Herein, we report the synthesis, spectroscopic characterization of eight new imidazole based mononuclear palladium(II) complexes (**1**–**8**). We also report the crystal structure of the complexes, dichlorobis(1-phenylimidazole) palladium(II) (**1**) and dibromobis(1-(4-methoxyphenyl)-1*H*-imidazole)palladium(II) (**6**) using single-crystal X-ray diffractometry (XRD). We also discuss their comparative catalytic activities in

* Corresponding authors. Tel.: +91 0 9811730475 (M. Trivedi), +1 314 516 5333 (N.P. Rath).
E-mail addresses: manojtri@gmail.com (M. Trivedi), rathn@umsl.edu (N.P. Rath).

0020-1693/$ - see front matter © 2012 Elsevier B.V. All rights reserved.
http://dx.doi.org/10.1016/j.ica.2012.08.003

the Mizoroki–Heck reaction [62,63] and the Suzuki–Miyaura coupling reaction [64–67].

2. Experimental

2.1. Materials and physical measurements

All the synthetic manipulations were performed under ambient atmosphere. The solvents were dried and distilled before use following the standard procedures. 1-(4-Methoxyphenyl)-1*H*-imidazole (Aldrich), 1-phenyl imidazole (Aldrich), 4(5)-(hydroxymethyl)-imidazole (Aldrich), Palladium chloride (Aldrich) and Palladium bromide (Aldrich) were used as received. $[PdX_2(MeCN)_2]$ and $[PdX_2(PhCN)_2]$, were prepared by Kharash's method and purified following the literature procedure [68]. The ligand 1-(4-cyanophenyl)-imidazole was prepared and purified following the literature procedures [69]. Elemental analyses were performed on a Carlo Erba Model EA-1108 elemental analyzer and data of C, H and N is within ±0.4% of calculated values. IR(KBr) and electronic spectra were recorded using Perkin-Elmer FT-IR spectrophotometer and Perkin Elmer Lambda-35 spectrometer, respectively. FAB mass spectra were recorded on a JEOL SX 102/DA 6000 mass spectrometer using Xenon (6 kV, 10 mA) as the FAB gas. The accelerating voltage was 10 kV and the spectra were recorded at room temperature with *m*-nitrobenzyl alcohol as the matrix. The ^1H and ^{13}C NMR spectra were recorded on a JEOL DELTA2 spectrometer at 400 MHz using TMS as an internal standard. The chemical shift values were recorded on the δ scale and the coupling constants (J) are in Hz. GCMS studies were done with the Shimadzu-2010 instrument containing a DB-5/RtX-5MS-30Mt and 60Mt column of 0.25 mm internal diameter. M^+ is the mass of the cation. The structural characterization of the recovered catalyst after one catalytic cycle was done using X-ray diffraction (XRD) measurements using Bruker D8 Discover X-ray diffractometer, with Cu $K\alpha_1$ radiation (λ = 1.5405 Å). Small quantities of the recovered catalyst after one catalytic cycle were dispersed in ethanol by sonicating for about 30 min. 5 ml of the suspension was put on copper grids using a microliter pipette for TEM measurements that was carried out using a FEI TECNAI G2 200 kV transmission electron microscope.

2.2. Synthesis of complexes

2.2.1. trans-[$PdCl_2(PI)_2$] (**1**)

This complex was prepared by the following two methods: (a) 1-phenylimidazole (0.288 g, 2 mmol) was added slowly to a solution of $[PdCl_2(CH_3CN)_2]$ (0.259 g, 1 mmol) in 30 mL CH_3OH:CH_2Cl_2 (50:50 V/V) mixture at room temperature. The resulting mixture was refluxed with stirring at room temperature for 24 h, during this the color of the solution changed from light yellow to dark yellow. The resulting solution was filtered and left at room temperature for slow evaporation crystallization. After three days, yellow color crystals were separated, washed with diethyl ether and dried. Yield: (0.325 g, 70%). *Anal.* Calc. for $C_{18}H_{16}Cl_2N_4Pd$: C, 46.45; H, 3.44; N, 12.04. Found: C, 46.66; H, 3.56; N, 12.34. IR(cm^{-1}, Nujol):ν = 3422, 3142(C—H), 3011, 2923, 2853, 2359, 2341, 1636(C=N), 1597, 1513, 1457, 1384, 1306, 1277, 1233, 1159, 1129(C—N), 1095, 1062, 1000, 966, 819, 766, 738(C—H), 692, 668, 653, 610, 530. Far-IR:ν (Pd—Cl) = 353 cm^{-1}. ^1H NMR (δ ppm, 400 MHz, $CDCl_3$, 298 K): 8.40(s, 2H, Imd), 7.60(d, 2H, J = 1.3 Hz, Imd), 7.37–7.53(m, 10H, J = 6.7 Hz, Ph), 7.15(t, 2H, J = 2.0 Hz, Imd). $^{13}C\{^1H\}$ NMR ($CDCl_3$): 137.60(C—Imd), 135.90(C—Ph), 129.10(C—Ph), 128.60(C—Ph), 125.60(C—Imd), 122.30(C—Imd). UV–Vis: λ_{max} (DMSO, ε[dm^3 mol^{-1} cm^{-1}]) = 342 (10976), 260 (8404). FAB-MS *m/z* 465(464), $[M]^+$; 429(430), $[M]^+$—Cl; 393(391), $[M]^+$—Cl_2.

(b) It was also prepared by the same method as described above except that $[PdCl_2(C_6H_5CN)_2]$ (0.383 g, 1 mmol) was used in place of $[PdCl_2(CH_3CN)_2]$. Yield: (0.372 g, 80%).

2.2.2. trans-[$PdCl_2(MPI)_2$] (**2**)

This complex was prepared by the following two methods: (a) 1-(4-methoxyphenyl)-1H-imidazole (0.348 g, 2 mmol) was added slowly to a solution of $[PdCl_2(CH_3CN)_2]$ (0.259 g, 1 mmol) in 30 mL CH_3OH:CH_2Cl_2 (50:50 V/V) mixture at room temperature. The resulting mixture was refluxed with stirring at room temperature for 24 h, during this the color of the solution changed from light yellow to dark yellow. The resulting solution was filtered and left at room temperature for slow evaporation crystallization. After 2 weeks, yellow color powder was separated, washed with diethyl ether and dried. Yield: (0.383 g, 73%). *Anal.* Calc. for $C_{20}H_{20}Cl_2N_4O_2Pd$: C, 45.71; H, 3.81; N, 10.67. Found: C, 45.80; H, 3.96; N, 10.80. IR(cm^{-1}, Nujol):ν = 3424, 3129, 3092, 2933, 2834, 1609(C=N), 1564, 1519, 1440, 1413, 1381, 1361, 1337, 1307, 1251, 1184, 1133(C—N), 1099, 1067, 1027, 955, 831, 810, 797, 730, 690, 666, 615, 524. Far-IR: ν (Pd—Cl) = 354 cm^{-1}. ^1H NMR (δ ppm, 400 MHz, $CDCl_3$, 298 K): 7.65–7.74(m, 6H, J = 6.5 Hz, Imd), 7.39–7.44(m, 8H, J = 7.5 Hz, Ph), 3.49(s, 6H, OCH_3). $^{13}C\{^1H\}$ NMR ($CDCl_3$): 158.80(C—Ph), 136.10(C—Imd), 129.30(C—Ph), 124.80(C—Imd), 123.10(C—Imd), 122.60(C—Ph), 114.20(C—Ph) 54.60(C—OCH_3). UV–Vis: λ_{max} (DMSO, ε[dm^3 mol^{-1} cm^{-1}]) = 343 (10630), 260 (8449). FAB-MS *m/z* 525(524), $[M]^+$; 489(491), $[M]^+$—Cl; 453(451), $[M]^+$ —Cl_2.

(b) It was also prepared by the same method as described above except that $[PdCl_2(C_6H_5CN)_2]$ (0.383 g, 1 mmol) was used in place of $[PdCl_2(CH_3CN)_2]$. Yield: (0.367 g, 70%).

2.2.3. trans-[$PdCl_2(HMI)_2$] (**3**)

This complex was prepared by the following two methods: (a) 4(5)-(hydroxylmethyl)imidazole (0.196 g, 2 mmol) was added slowly to a solution of $[PdCl_2(CH_3CN)_2]$ (0.259 g, 1 mmol) in 30 mL CH_3OH:CH_2Cl_2 (50:50 V/V) mixture at room temperature. The resulting mixture was refluxed with stirring at room temperature for 24 h, during this the color of the solution changed from light yellow to light greenish yellow. The resulting solution was filtered and left at room temperature for slow evaporation crystallization. After two weeks, yellow color powder was separated, washed with diethyl ether and dried. Yield: (0.280 g, 75%). *Anal.* Calc. for $C_8H_{12}Cl_2N_4O_2Pd$: C, 25.73; H, 3.22; N, 15.01. Found: C, 25.80; H, 3.36; N, 15.30. IR(cm^{-1}, Nujol):ν = 3420, 3100(OH), 2926, 2850, 1640, 1590(C=N), 1458, 1380, 1304, 1284, 1150, 1130(C—N), 1090, 1040, 1006, 968, 820, 770, 740, 691, 660, 650, 615, 516. Far-IR: ν (Pd—Cl) = 353 cm^{-1}. ^1H NMR (δ ppm, 400 MHz, DMSO-d_6, 298 K): 7.57(s, 2H, Imd), 6.90(s, 2H, Imd), 4.43(s, 4H, CH_2OH). $^{13}C\{^1H\}$ NMR ($CDCl_3$): 136.80(C—Imd), 135.40(C—Imd), 120.80(C—Imd), 62.80(C—CH_2OH). UV–Vis: λ_{max} (DMSO, ε[dm^3 mol^{-1} cm^{-1}]) = 366 (7688), 260 (7814). FAB-MS *m/z* 373(371), $[M]^+$; 337(336), $[M]^+$—Cl; 301(307), $[M]^+$—Cl_2.

(b) It was also prepared by the same method as described above except that $[PdCl_2(C_6H_5CN)_2]$ (0.383 g, 1 mmol) was added in place of $[PdCl_2(CH_3CN)_2]$. Yield: (0.223 g, 60%).

2.2.4. trans-[$PdCl_2(CPI)_2$] (**4**)

This complex was prepared by the following two methods: (a) CPI (0.338 g, 2 mmol) was added slowly to a solution of $[PdCl_2(CH_3CN)_2]$ (0.259 g, 1 mmol) in 30 mL CH_3OH:CH_2Cl_2 (50:50 V/V) mixture at room temperature. The resulting mixture was stirred at room temperature for 24 h, during this the color of the solution changed from light yellow to dark turbid yellow. Finally, the yellow color solid precipitated out, and was filtered, washed with diethyl

ether and dried. Yield: (0.412 g, 80%). *Anal.* Calc. for $C_{20}H_{14}Cl_2N_6Pd$: C, 46.60; H, 2.72; N, 16.31. Found: C, 46.90; H, 2.96; N, 16.46. IR(cm^{-1}, Nujol):ν = 3407, 3147, 2922, 2225(CN), 1608(C=N), 1522, 1384, 1306, 1102(C—N), 1059, 962, 835, 723, 643, 622, 573, 547. Far-IR:ν = 341 cm^{-1}. ^{1}H NMR (δ ppm, 400 MHz, $CDCl_3$, 298 K): 8.38(s, 2H, Imd), 8.16(d, 2H, J = 8.7 Hz, Imd), 7.83(d, 2H, J = 4.5 Hz, Imd), 7.73(d, 4H, J = 7.5 Hz, CNPh), 7.48(d, 4H, J = 6.0 Hz, CNPh). $^{13}C\{^1H\}$ NMR ($CDCl_3$): 136.40(C—Imd), 132.90 (C—CNPh), 129.30(C—CNPh), 127.20(C—CNPh), 124.40(C—CNPh), 124.20(C—Imd), 123.60(C—Imd), 113.12(CN—CNPh). UV–Vis: λ_{max} (DMSO, ε[dm^3 mol^{-1} cm^{-1}]) = 335 (23902), 265 (16643). FAB-MS *m/z*515(516), $[M]^+$; 479(480), $[M]^+$—Cl; 443(441), $[M]^+$—Cl_2.

(b) It was also prepared by the same method as described above except that $[PdCl_2(C_6H_5CN)_2]$ (0.383 g, 1 mmol) was added in place of $[PdCl_2(CH_3CN)_2]$. Yield: (0.283 g, 55%).

2.2.5. trans-[$PdBr_2$(PI)$_2$] (**5**)

This complex was prepared by the following two methods: (a) 1-phenylimidazole (0.288 g, 2 mmol) was added slowly to a solution of $[PdBr_2(CH_3CN)_2]$ (0.348 g, 1 mmol) in 30 mL CH_3OH:CH_2Cl_2 (50:50 V/V) mixture at room temperature. The resulting mixture was stirred at room temperature for 24 h, during this the color of the solution changed from light yellow to greenish yellow. The resulting solution was filtered and left at room temperature for slow evaporation crystallization. After two weeks, greenish yellow color powder was separated, washed with diethyl ether and dried. Yield: (0.470 g, 85%). *Anal.* Calc. for $C_{18}H_{16}Br_2N_4Pd$: C, 38.98; H, 2.88; N, 10.11. Found: C, 39.10; H, 2.94; N, 10.26. IR(cm^{-1}, Nujol):ν = 3418, 3112(C—H), 3010, 2926, 2851, 1610(C=N), 1580, 1500, 1430, 1380, 1304, 1260, 1150, 1120(C—N), 1080, 1000, 946, 888, 750, 725(C—H), 680, 670, 643, 600, 510. Far-IR:ν (Pd—Br) = 245 cm^{-1}. ^{1}H NMR (δ ppm, 400 MHz, $CDCl_3$, 298 K): 8.38(s, 2H, Imd), 7.50(d, 2H, J = 3.0 Hz, Imd), 7.33–7.48(m, 10H, J = 7.5 Hz, Ph), 7.20(t, 2H, J = 4.5 Hz, Imd). $^{13}C\{^1H\}$ NMR ($CDCl_3$): 136.40(C—Imd), 135.20(C—Ph), 129.05(C—Ph), 128.40(C—Ph), 125.30(C—Imd), 122.10(C—Imd). UV–Vis: λ_{max} (DMSO, ε[dm^3 mol^{-1} cm^{-1}]) = 389 (6172), 260 (15781). FAB-MS *m/z* 554(555), $[M]^+$; 474(476), $[M]^+$—Br; 394(395), $[M]^+$—Br_2.

(b) It was also prepared by the same method as described above except that $[PdBr_2(C_6H_5CN)_2]$ (0.472 g, 1 mmol) was added in place of $[PdBr_2(CH_3CN)_2]$. Yield: (0.415 g, 75%).

2.2.6. trans-[$PdBr_2$(MPI)$_2$] (**6**)

This complex was prepared by the following two methods: (a) 1-(4-methoxyphenyl)-1H-imidazole (0.348 g, 2 mmol) was added slowly to a solution of $[PdBr_2(CH_3CN)_2]$ (0.348 g, 1 mmol) in 30 mL CH_3OH:CH_2Cl_2 (50:50 V/V) mixture at room temperature. The resulting mixture was stirred at room temperature for 24 h, during this the color of the solution changed from reddish orange to dark orange. The resulting solution was filtered and left at room temperature for slow evaporation crystallization. After two weeks, orange color crystals were separated, washed with diethyl ether and dried. Yield: (0.368 g, 60%). *Anal.* Calc. for $C_{20}H_{20}Br_2N_4O_2Pd$: C, 39.08; H, 3.26; N, 9.12. Found: C, 39.28; H, 3.26; N, 9.10. IR(cm^{-1}, Nujol):ν = 3309, 3220, 1625(C=N), 1585, 1497, 1449, 1385, 1353, 1273, 1240, 1088(C—N), 1003, 832, 749, 725, 660, 640, 610, 515. Far-IR: ν (Pd—Br) = 244 cm^{-1}. ^{1}H NMR (δ ppm, 400 MHz, $CDCl_3$, 298 K): 7.68–7.73(m, 6H, J = 5.5 Hz, Imd), 7.38–7.43(m, 8H, J = 7.1 Hz), 3.49(s, 6H, OCH_3). $^{13}C\{^1H\}$ NMR ($CDCl_3$): 157.40(C—Ph), 136.30(C—Imd), 129.10(C—Ph), 124.40(C—Imd), 123.10(C—Imd), 122.40(C—Ph), 114.10(C—Ph) 54.30(C—OCH_3). UV–Vis: λ_{max} (DMSO, ε[dm^3 mol^{-1} cm^{-1}]) = 340 (23162), 261 (15253). FAB-MS *m/z* 614(616), $[M]^+$; 534(533), $[M]^+$—Br; 454(453), $[M]^+$—Br_2.

(b) It was also prepared by the same method as described above except that $[PdBr_2(C_6H_5CN)_2]$ (0.472 g, 1 mmol) was added in place of $[PdBr_2(CH_3CN)_2]$. Yield: (0.429 g, 70%).

2.2.7. trans-[$PdBr_2$(HMI)$_2$] (**7**)

This complex was prepared by the following two methods: (a) 4(5)-(Hydroxyl methyl)imidazole (0.196 g, 2 mmol) was added slowly to a solution of $[PdBr_2(CH_3CN)_2]$ (0.348 g, 1 mmol) in 30 mL CH_3OH:CH_2Cl_2 (50:50 V/V) mixture at room temperature. The resulting mixture was stirred at room temperature for 24 h, during this the color of the solution changed from greenish yellow to orange. The resulting solution was filtered and left at room temperature for slow evaporation crystallization. After two weeks, mustard yellow color powder was separated, washed with diethyl ether and dried. Yield: (0.300 g, 71%). *Anal.* Calc. for $C_8H_{12}Br_2N_4O_2$-Pd: C, 20.78; H, 2.59; N, 12.12. Found: C, 20.80; H, 2.86; N, 12.36. IR(cm^{-1}, Nujol):ν = 3420, 3100(OH), 2926, 2850, 1640(C=N), 1590, 1458, 1380, 1304, 1284, 1150, 1130(C—N), 1090, 1040, 1006, 968, 820, 770, 740, 691, 660, 650, 615, 516. Far-IR: ν (Pd—Br) = 245 cm^{-1}. ^{1}H NMR (δ ppm, 400 MHz, DMSO-d_6, 298 K): 7.56(s, 2H, Imd), 6.91(s, 2H, Imd), 4.44(s, 4H, CH_2OH). $^{13}C\{^1H\}$ NMR ($CDCl_3$): 136.30(C—Imd), 135.10(C—Imd), 120.50(C—Imd), 62.30(C—CH_2OH). UV–Vis: λ_{max} (DMSO, ε[dm^3 mol^{-1} cm^{-1}]) = 354 (15460), 261 (7855). FAB-MS *m/z* 462(466), $[M]^+$; 382(384), $[M]^+$—Br; 302(307), $[M]^+$—Br_2.

(b) It was also prepared by the same method as described above except that $[PdBr_2(C_6H_5CN)_2]$ (0.472 g, 1 mmol) was added in place of $[PdBr_2(CH_3CN)_2]$. Yield: (0.446 g, 65%).

2.2.8. trans-[$PdBr_2$(CPI)$_2$] (**8**)

This complex was prepared by the following two methods: (a) CPI (0.338 g, 2 mmol) was added slowly to a solution of $[PdBr_2(CH_3CN)_2]$ (0.348 g, 1 mmol) in 30 mL CH_3OH:CH_2Cl_2 (50:50 V/V) mixture at room temperature. The resulting mixture was stirred at room temperature for 24 h, during this the color of the solution changed from light orange to dark orange. Finally, the orange color solid precipitated out, and was filtered, washed with diethyl ether and dried. Yield: (0.483 g, 80%). *Anal.* Calc. for $C_{20}H_{14}Br_2N_6Pd$: C, 39.74; H, 2.32; N, 13.91. Found: C, 39.82; H, 2.46; N, 13.90. IR(cm^{-1}, Nujol):ν = 3407, 3148, 2916, 2225(CN), 1608(C=N), 1522, 1493, 1428, 1372, 1338, 1306, 1254, 1185, 1131(C—N), 1103, 1059, 1027, 962, 836. Far-IR:ν = 341 cm^{-1}. ^{1}H NMR (δ ppm, 400 MHz, $CDCl_3$, 298 K): 8.40(s, 2H, Imd), 8.20(d, 2H, J = 8.7 Hz, Imd), 7.81(d, 2H, J = 4.5 Hz, Imd), 7.71(d, 4H, J = 7.5 Hz, CNPh), 7.45 (d, 4H, J = 6.0 Hz, CNPh). $^{13}C\{^1H\}$ NMR ($CDCl_3$): 136.10(C—Imd), 132.60(C—CNPh), 129.10(C—CNPh), 127.40(C—CNPh), 124.30(C—CNPh), 124.10(C—Imd), 123.30 (C—Imd), 112.90(CN—CNPh). UV–Vis: λ_{max} (DMSO, ε[dm^3 mol^{-1} cm^{-1}]) = 340 (3550), 273 (27109). FAB-MS *m/z* 604(604), $[M]^+$; 524(525), $[M]^+$—Br; 444(446), $[M]^+$—Br_2.

(b) It was also prepared by the same method as described above except that $[PdBr_2(C_6H_5CN)_2]$ (0.472 g, 1 mmol) was added in place of $[PdBr_2(CH_3CN)_2]$. Yield: (0.392 g, 65%).

2.3. X-ray crystallographic study

Intensity data for **1**, and **6** were collected on X-calibur S oxford, Bruker APEXII and Enraf–Nonius MACH3 CCD area detector diffractometers using graphite monochromatized Mo Kα radiation at 293(2) and 100(2) K and 150(2) K (**6**). SMART and SAINT software packages [70] were used for data collection and data integration for **1**, and **6**. Structure solution and refinement were carried out using the SHELXTL-PLUS software package [71,72]. The non-hydrogen atoms were refined with anisotropy thermal parameters. All the hydrogen atoms were treated using appropriate riding models. The computer programme PLATON was used for analyzing the interaction and stacking distances [71,72].

2.4. Catalytic reactions

2.4.1. General procedure for Mizoroki–Heck reaction

K_2CO_3 (553 mg, 4.0 mmol) was added to a 100 ml three-necked flask with a stirring bar and the flask was dried under vacuum and then filled with nitrogen, aryl halide or 4-halotolune (2.0 mmol) and *n*-butylacrylate or styrene (2.0 mmol) in DMF (10 mL). Then 0.001 equivalent palladium complex in DMF was added *via* a syringe under nitrogen atmosphere. The mixture was stirred at 140 °C for the indicated reaction time. After the completion of the reaction, the mixture was cooled, the precipitate was removed by filtration and the product was extracted from the filtrate with diethyl ether. The combined organic layer was dried over anhydrous Na_2SO_4 and filtered. After evaporation, the obtained residue was purified by silica-gel column chromatography to give the Mizoroki–Heck product. Product identities were confirmed by ^1H and ^{13}C NMR and GC–MS.

2.4.2. General procedure for Suzuki coupling reaction

K_2CO_3 (553 mg, 4.0 mmol) was added to a 100 ml three-necked flask with a stirring bar and the flask was dried under vacuum and then filled with nitrogen, aryl halide or 4-halotolune (2.0 mmol) and phenylboronic acid (244.0 mg, 2.0 mmol) in DMF (10 mL). Then 0.001 equivalent palladium complex in DMF was added *via* a syringe under nitrogen atmosphere. The mixture was stirred at 120 °C for the indicated reaction time. The mixture was cooled and the precipitate was removed by filtration and the product was extracted from the filtrate with diethyl ether. The combined organic layer was dried over anhydrous Na_2SO_4 and filtered. After evaporation, the obtained residue was purified by silica-gel column chromatography to give the coupling product. Product identities were confirmed by ^1H and ^{13}C NMR and GC–MS.

2.4.3. Procedure of Hg poisoning experiments for Mizoroki–Heck reaction

An excess of Hg(0) (300 equivalent relative to *trans*-$[PdX_2L_2]$) was added into the reaction mixture of aryl halide or 4-halotolune (2.0 mmol), *n*-butylacrylate or styrene (2.0 mmol), K_2CO_3 (553 mg, 4.0 mmol), and complexes **1**–**8** (0.001 equivalent) in DMF (10 mL) at t = 0, 24 h, respectively.

2.4.4. Procedure of Hg poisoning experiments for Suzuki coupling reaction

An excess of Hg(0) (300 equivalent relative to *trans*-$[PdX_2L_2]$) was added into the reaction mixture of aryl halide or 4-halotolune (2.0 mmol), phenylboronic acid (244.0 mg, 2.0 mmol), K_2CO_3 (553 mg, 4.0 mmol), and complexes **1**–**8** (0.001 equivalent) in DMF (10 mL) at t = 0, 24 h, respectively.

3. Results and discussion

3.1. Synthesis

Reaction of the $[PdX_2(RCN)_2]$ [where X = Cl, Br; R = CH_3—, C_6H_5—] with L in 1:2 stoichiometric ratio in a mixture of dichloromethane and methanol (1:1v/v) under stirring at RT afforded neutral mononuclear *trans*-complexes with the formulations $[PdX_2L_2]$ (**1**–**8**) in good yield (Scheme 1).

3.2. Characterization

All the complexes were isolated as air-stable, non-hygroscopic solids and soluble in dimethylformamide, dimethylsulfoxide and halogenated solvents like chloroform but insoluble in petroleum ether and diethyl ether and do not show any signs of decomposition in solution upon exposure to air for days. Information about the composition of the complexes and structure and bonding has been derived from the analytical spectral studies. Analytical data of the complexes conformed well to their respective formulations. More information about composition of the complexes was also obtained from FAB-MS. Resulting data is recorded in the experimental section and representative FAB-MS spectrum of the neutral complex **3** and **7** are shown in F-1, Supporting material. The positions of different peaks and overall fragmentation patterns in the FAB-MS of the respective complexes are consistent with their formulations.

The IR spectra of all mononuclear complexes **1**–**8**, exhibited identical bands in the region 3300–3100 cm^{-1} [υ(N—H) and/or υ(C—H)], 1580–1500 cm^{-1} [ring stretching or δ(N—H)], 1290–1260 cm^{-1} (in plane C—H bending), 912–888 cm^{-1} (ring vibration), 750–725 cm^{-1} (out-of plane C—H bending), 680–670 cm^{-1} (ring stretch/bending) and 630–600 cm^{-1} (ring deformation) (See F-2, Supporting material). The mononuclear complexes **4** and **8**, displayed sharp and intense bands around 2225–2227 cm^{-1} corresponding to ν(C≡N) (See F-3, Supporting material). The position of the ν(C≡N) remained unaltered, compared to that in the ligand itself, it suggested linkage of CPI with the palladium centre in the respective complexes through imidazole nitrogen. The Far-IR spectra of all the complexes reveal a strong absorbtion band at 353–354 cm^{-1} for PdL_2Cl_2 compounds and at 244–245 cm^{-1} for PdL_2Br_2 compounds. The former band may be assigned to υ(Pd—Cl) (See F-4, Supporting material) while the latter to υ(Pd—Br) stretch. These

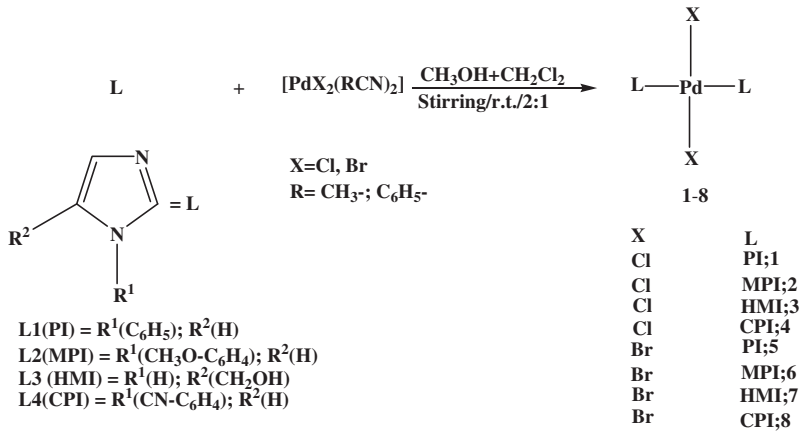

Scheme 1. Graphical representation for synthesis of **1**–**8**.

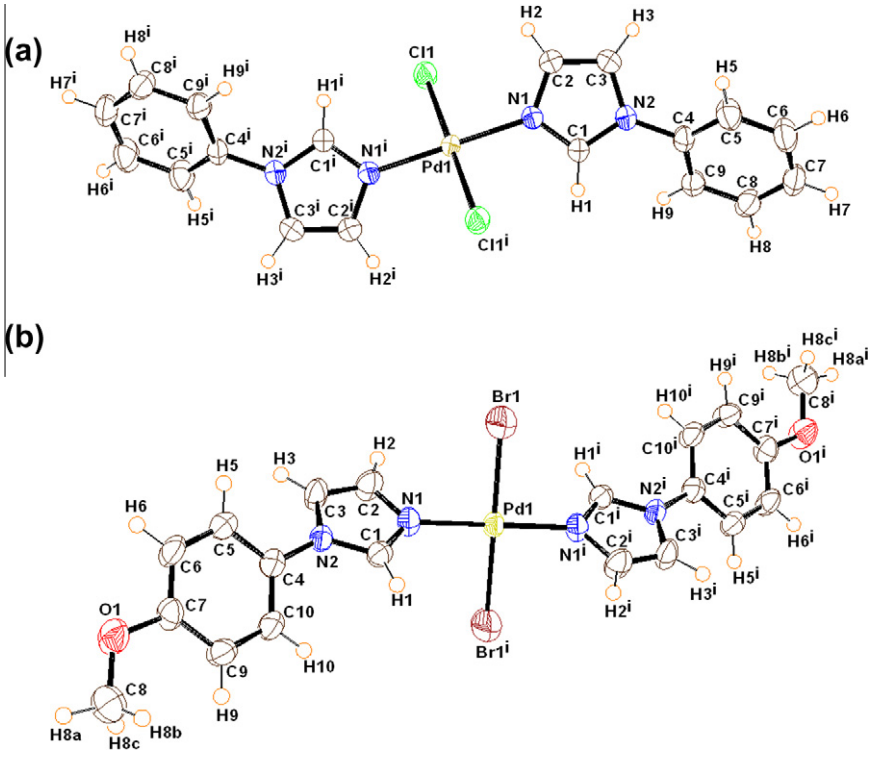

Fig. 1. Molecular structures for (a) **1**, and (b) **6** (30% thermal ellipsoids are shown).

Table 1
Crystallographic data for Complexes **1** and **6**.

	1	**6**
Formula	$C_{18}H_{16}Cl_2N_4Pd$	$C_{20}H_{20}Br_2N_4O_2Pd$
Formula weight	465.65	614.62
T (K)	100(2)	150(2)
Crystal system	triclinic	monoclinic
Space group	$P\bar{1}$	$P2_1/c$
a (Å)	7.0872(4)	11.1921(3)
b (Å)	7.8015(5)	12.3378(3)
c (Å)	9.4730(6)	7.7358(2)
α (°)	106.659(3)	90
β (°)	99.131(3)	91.103(2)
γ (°)	115.376(3)	90
V (Å^3)	428.72(5)	1068.01(5)
Z	1	2
D_{calc} (g cm^{-3})	1.804	1.911
μ (mm^{-1})	1.402	4.634
Goodness-of-fit (GOF) on F^2	1.072	1.121
R_1 all	0.0232	0.0609
R_1 [$I > 2\sigma(I)$]	0.0221	0.0518
wR_2	0.0483	0.1757
wR_2 [$I > 2\sigma(I)$]	0.0478	0.1705
GOF on F^2	1.072	1.121

Table 2
Selected bond lengths (Å), and bond angles (°) for complexes **1** and **6**.

Complex-**1**		Complex-**6**	
Pd(1)—Cl(1)	2.2954(2)	Pd(1)—Br(1)	2.3842(10)
Pd(1)—Cl(1)$^{\#1}$	2.2954(2)	Pd(1)—Br(1)$^{\#1}$	2.3842(10)
Pd(1)—N(1)	2.0088(7)	Pd(1)—N(1)	2.007(5)
Pd(1)—N(1)$^{\#1}$	2.0088(7)	Pd(1)—N(1)$^{\#1}$	2.007(5)
N(1)—C(1)	1.3809(11)	O(1)—C(7)	1.378(8)
N(1)—C(3)	1.3199(11)	O(1)—C(8)	1.405(10)
N(2)—C(3)	1.3483(11)	N(1)—C(1)	1.330(9)
N(2)—C(2)	1.3822(11)	N(1)—C(2)	1.358(9)
N(2)—C(4)	1.4263(11)	N(2)—C(1)	1.346(9)
N(1)$^{\#1}$—Pd(1)—N(1)	180.00(6)	N(2)—C(3)	1.371(9)
N(1)$^{\#1}$—Pd(1)—Cl(1)	89.94(2)	N(2)—C(4)	1.433(9)
N(1)—Pd(1)—Cl(1)	90.06(2)	N(1)$^{\#1}$—Pd(1)—N(1)	180.000(1)
N(1)$^{\#1}$—Pd(1)—Cl(1)$^{\#1}$	90.06(2)	N(1)$^{\#1}$—Pd(1)—Br(1)	90.56(17)
N(1)—Pd(1)—Cl(1)$^{\#1}$	89.94(2)	N(1)—Pd(1)—Br(1)	89.44(17)
Cl(1)—Pd(1)—Cl(1)$^{\#1}$	180.000(1)	N(1)$^{\#1}$—Pd(1)—Br(1)$^{\#1}$	89.44(17)
C(3)—N(1)—Pd(1)	125.85(6)	N(1)—Pd(1)—Br(1)$^{\#1}$	90.56(17)
C(1)—N(1)—Pd(1)	127.30(6)	Br(1)—Pd(1)—Br(1)$^{\#1}$	180.0
C(3)—N(1)—C(1)	106.83(7)	C(7)—O(1)—C(8)	117.5(6)
C(3)—N(2)—C(2)	107.63(7)	C(1)—N(1)—C(2)	106.6(6)
C(3)—N(2)—C(4)—C(9)	43.91(13)	C(1)—N(1)—Pd(1)	127.2(5)
C(2)—N(2)—C(4)—C(9)	−132.50(10)	C(2)—N(1)—Pd(1)	126.1(5)
		C(1)—N(2)—C(4)—C(10)	−35.3(10)
		C(3)—N(2)—C(4)—C(5)	−33.5(10)

bands agree well with the *trans*-orientation of the halogens in the square planar palladium complexes [73].

The ^{1}H NMR spectral data of the complexes along with their assignments are recorded in the experimental section. In the ^{1}H NMR spectra of all the complexes **1**–**8**, imidazole protons displayed down field shift as compared to that in the ligand itself (See F-5 and F-6, Supporting material). Downfield shift in the position of the imidazole protons (8.40–6.90 ppm) might result from the change in electron density on the palladium center due to linkage of PI or MPI or HMI or CPI through its imidazole nitrogen. The conjugative and electron withdrawing abilities of the —CN/—C_6H_5/—OCH_3/—CH_2OH groups pulls electron density away from the imidazole ring towards itself, leading to a decrease of electron density on the palladium center which in turn, may pull more electron density away from the imidazole ring, leading to deshielding of imidazole protons. The ^{1}H NMR spectra of the Br containing complexes show little change on coordination with imidazole based ligands. The position and integrated intensity of various resonances supported well the presence of ligand and formulation of the respective complexes. In the ^{13}C NMR spectra of the complexes **2**, **6**, and **3**, **7** show peaks for —OCH_3 and —CH_2OH carbon of the MPI and HMI at δ = 54.30–54.60 and 62.30–62.80 ppm,

Table 3
Hydrogen bond parameters for **1** and **6**.

D—H···A—X	*d* H···A Å	*D* D···A (Å)	*θ* D—H···A (°)
Complex ***1***			
C(3)—H(3)···Cl(1)[a]	2.80	3.1771	105
Complex ***6***			
C(1)—H(1)···O(1)[b]	2.47	3.340(8)	153
C(5)—H(5)···Br(1)[c]	2.73	3.636(7)	160

Symmetry equivalents:
[a] 2 − *x*, 1 − *y*, −*z*.
[b] −*x*, 1/2 + *y*,1/2 − *z*.
[c] 1 − *x*, −1/2 + *y*, 1/2−*z*.

respectively. The nitrile carbon of the CPI in the complexes **4** and **8** resonated at 112.90–113.12 ppm, while the other carbons of CPI resonated in the range 123.30–136.40 ppm.

3.3. Molecular structure determination

Molecular structure of the complexes **1** and **6** with atomic numbering scheme is shown in Fig. 1. Details about the data collection, solution and refinement are presented in Table 1 and selected bond lengths and bond angles and hydrogen bond parameters are tabulated in Table 2 and 3, respectively. Complex **1** and **6** crystallized in triclinic and monoclinic system with *P*1 and $P2_1/c$ space group. The asymmetric unit in complex **1** and **6** comprises half of the formula unit in the solid state. The coordination geometry of the complexes **1** and **6** show an almost ideal square planar environment, with N(1)—Pd(1)—Cl(1), N(1)—Pd(1)—Cl(1)$^{\#1}$, N(1)—Pd(1)—Br(1)and N(1)—Pd(1)—Br(1)$^{\#1}$ angles of 90.06(2)°, 89.94(2)°, 89.44(17)°, and 90.56(17)°, respectively. The angles between the N(1)$^{\#1}$—Pd(1)—N(1), Cl(1)—Pd(1)—Cl(1)$^{\#1}$, N(1)$^{\#1}$—Pd(1)—N(1) and Br(1)—Pd(1)—Br(1)$^{\#1}$ bonds are 180.00(6)°, 180.000(1)°, 180.000(1)° and 180.0°, respectively which indicated that the 1-phenyl imidazole or 4-methoxyimidazole rings and the two chloride or bromide ions in the coordination sphere are found to be *trans* disposed. The Pd—Cl (2.2954(2) Å), Pd—Br (2.3842(10) Å) and Pd—N distances (2.007(5)–2.0088(7) Å) in **1**, and **6** lie in the range expected for such bonds. These are comparable to those in other Pd(II) imidazole complexes [45–57,58–61,74–78]. The C—O bond distances in **6** are 1.378(8)–1.405(10) Å, respectively. These are normal and comparable with C—O distances in other complexes [79]. The ligand 1-phenylimidazole or 4-methoxyimidazole has lost planarity upon coordination with metal center. The phenyl group of the ligand is not coplanar with imidazole ring and is tilted with respect to the imidazole ring plane at an angle of 44.7(3)–43.91(13)° in **1** and 35.3(10)–35.5(10)° in **6**. The inter annular bond distances N(2)—C(4) in **1**, and **6** are 1.434(3)–1.426(11) Å and 1.433(9) Å, respectively. These are slightly shorter than a single C—N bond indicating a double bond character. Crystal packing in **1** is stabilised by intermolecular C—H···π, inter- and intra-molecular C—H···Cl, and intra- and inter-molecular C—H···X (X = Cl, π) and π–π interactions, while in **6**, intra- and inter-molecular C—H···X (X = Br, O, π) and π–π

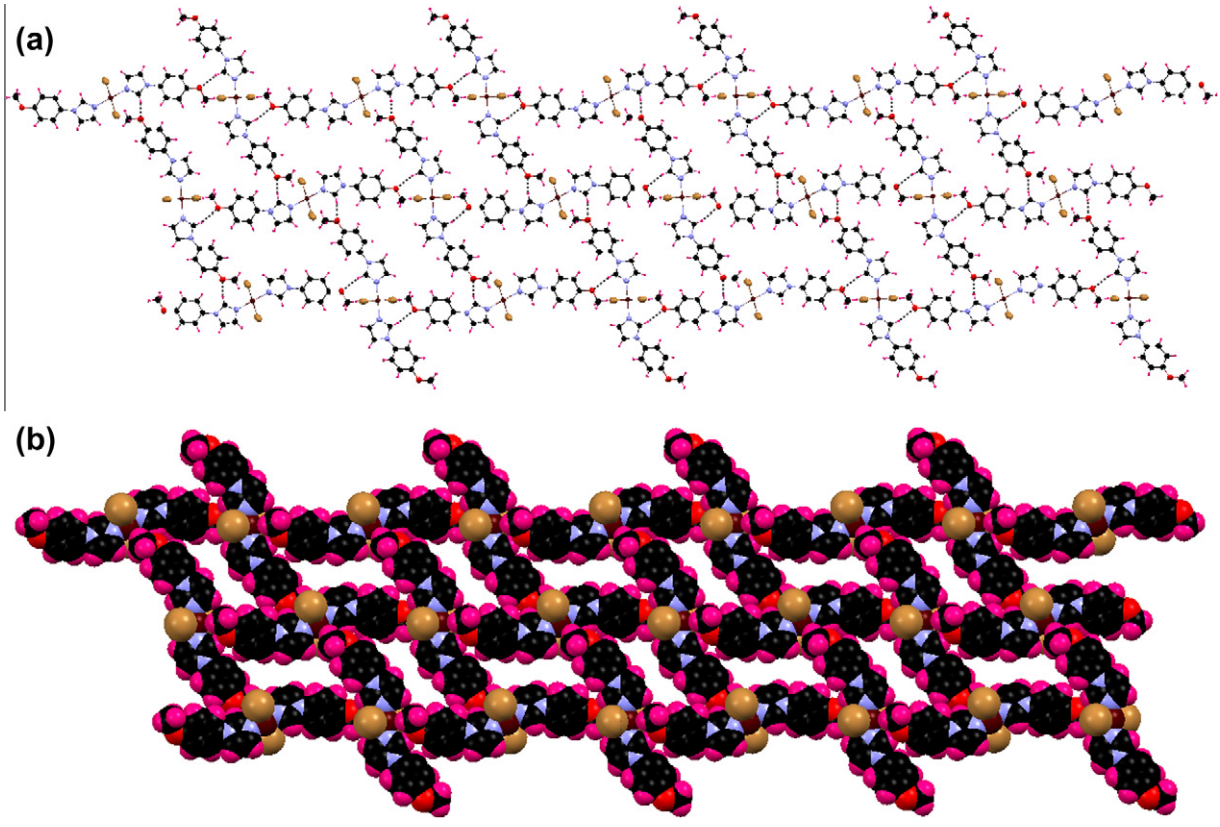

Fig. 2. Parallel channels motif in complex **6** accompanied by C—H···O interactions along crystallographic '*c*'-axis.

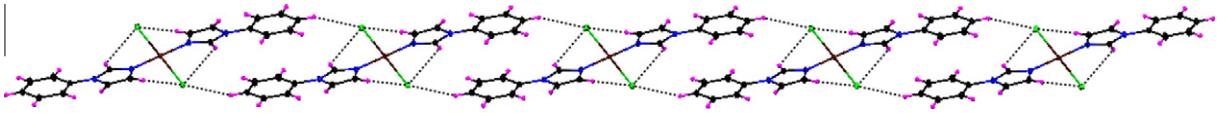

Fig. 3. Straight channels motif in complex **1** accompanied by C—H···Cl interactions.

Table 4
Results of the Mizoroki–Heck cross-coupling reactions of aryl halides with vinyl compounds using complex **1**–**8**[a].

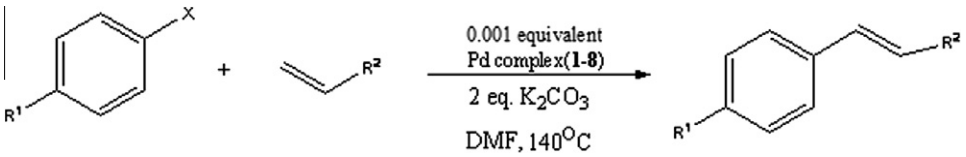

Entry	R^1	R^2	X	Yield (%)[b]/(TON)[c]							
				1	**2**	**3**	**4**	**5**	**6**	**7**	**8**
a	H	$CO_2{}^nBu$	Br	89 (890)	92 (920)	53 (530)	56 (560)	90 (900)	91 (910)	59 (590)	60 (600)
b	H	$CO_2{}^nBu$	I	88 (880)	85 (850)	60 (600)	66 (660)	90 (900)	87 (870)	64 (640)	61 (610)
c	H	$CO_2{}^nBu$	Cl	60 (600)	55 (550)	36 (360)	30 (300)	50 (500)	48 (480)	35 (350)	38 (380)
d	CH_3	$CO_2{}^nBu$	Br	100 (1000)	98 (980)	70 (700)	61 (610)	94 (940)	96 (960)	59 (590)	55 (550)
e	CH_3	$CO_2{}^nBu$	I	96 (960)	97 (970)	65 (650)	66 (660)	98 (980)	96 (960)	62 (620)	64 (640)
f	CH_3	$CO_2{}^nBu$	Cl	65 (650)	60 (600)	40 (400)	39 (390)	64 (640)	58 (580)	36 (360)	35 (350)
g	H	C_6H_5	Br	92 (920)	91 (910)	68 (680)	49 (490)	90 (900)	91 (910)	57 (570)	47 (470)
h	H	C_6H_5	I	92 (920)	90 (900)	47 (470)	56 (560)	91 (910)	92 (920)	65 (650)	67 (670)
i	H	C_6H_5	Cl	59 (590)	61 (610)	37 (370)	32 (320)	60 (600)	55 (550)	35 (350)	31 (310)
j	CH_3	C_6H_5	Br	93 (930)	94 (940)	62 (620)	62 (620)	95 (950)	97 (970)	60 (600)	60 (600)
k	CH_3	C_6H_5	I	95 (950)	98 (980)	63 (630)	66 (660)	99 (990)	93 (930)	61 (610)	64 (640)
l	CH_3	C_6H_5	Cl	70 (700)	65 (650)	40 (400)	41 (410)	71 (710)	66 (660)	35 (350)	37 (370)

[a] All reactions were carried out using 2.0 mmol activated or non-activated aryl halide, 2.0 mmol vinyl compound, 4.0 mmol K_2CO_3, 0.001 equivalent Pd complex and 10 ml DMF at 140 °C for 24 h.
[b] Isolated yield.
[c] Mol(substrate) X% yield/mol(Pd).

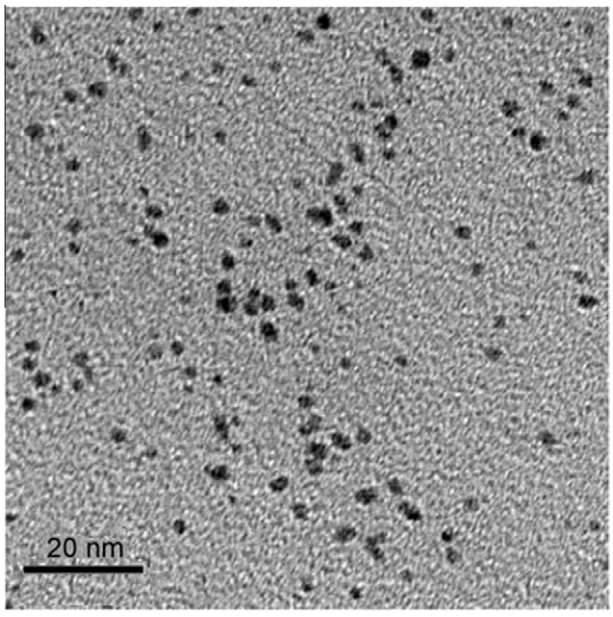

Fig. 4. TEM image of the recovered catalyst (**1**) after one catalytic cycle in the Heck reaction.

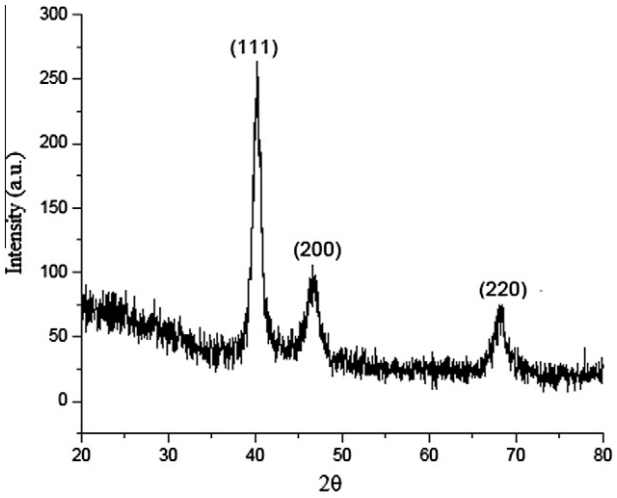

Fig. 5. XRD pattern of the recovered catalyst (**1**) after one catalytic cycle in the Heck reaction.

interactions are present. Packing in **6** along crystallographic '*c*'-axis through C—H···O interactions leading to parallel channels motif (Fig. 2). Contact distances for C—H···O interactions are 2.467 Å. C—H C—H···Cl type intra- and inter-molecular interactions result in the formation of straight channels motif both in **1** (Fig. 3). The inter- and intra-nuclear C—H···π interactions that are present in complex **1** result in single helical motif (See F-7, Supporting material). The most noteworthy structural feature of complex **1** is face-

Table 5
Effect of Hg(0) poisoning in the Mizoroki–Heck coupling reaction.[a]

Entry	R^1	R^2	X	Yield (%)[b]							
				1	**2**	**3**	**4**	**5**	**6**	**7**	**8**
a	CH_3	$CO2^nBu$	Br	2	3	70	61	5	4	59	55
b	CH_3	C_6H_5	Br	3	4	62	62	4	3	60	60

[a] All reactions were carried out using 2.0 mmol activated or non-activated aryl halide, 2.0 mmol vinyl compound, 4.0 mmol K_2CO_3, 0.001 equivalent Pd complex + 300 equivalent of Hg(0) and 10 ml DMF at 140 °C for 24 h.
[b] Isolated yield.

to-face π–π interactions between carbon atoms of the imidazole rings (See F-8, Supporting material). The contact distances for face-to-face interactions are 3.353–3.361Å. Inter-molecular C—H···Br interactions are present in **6** (See F-9, Supporting material). The C—H···Cl and C—H···Br contact distances are in the range of 2.48–2.94 Å. These distances are within the range reported in the literature [80]. The intra and inter-molecular C—H···π weak interactions are also present in **6** but only intra-molecular C—H···p interactions has been present in **1**. Contact distances for intra- and inter-C—H π interactions are in the range of 2.51–2.86 and 2.82 Å (See F-10, Supporting material). The importance of π–π stacking interactions between aromatic rings has been widely recognized in the intercalation of drugs with DNA which lie in the range of 3.4–3.5 Å. Complex **6** exhibit intermolecular face-to-face (πphenyl/πphenyl (ct/ct distances 3.382 Å) (See F-11, Supporting material).

3.4. Catalytic application of the complexes

3.4.1. Mizoroki–Heck reaction catalyzed by Pd complexes *1–8*

To compare the catalytic activities of complexes **1**–**8** in the Mizoroki–Heck reaction, we examined the reaction of activated or non-activated aryl halides and vinyl compounds in the presence of 0.001 equivalent Pd catalyst in DMF at 140 °C (Table 4). Recent discovery by de Vries [81] and Hayashi and co-workers [74] have proposed the role of Pd species in the Mizoroki–Heck reaction under high temperature, and they proposed the mechanism of

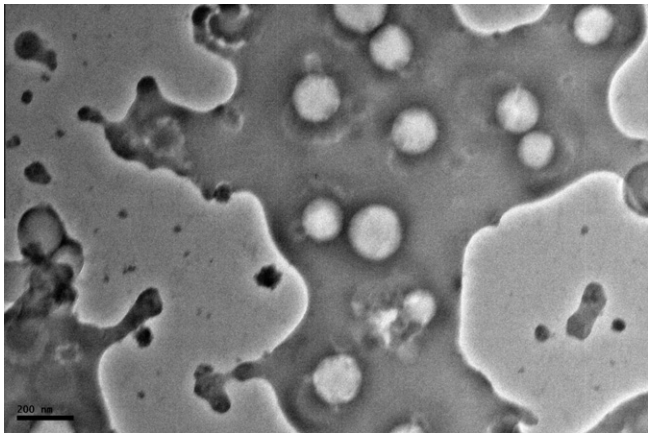

Fig. 6. TEM image of the recovered catalyst (**5**) after one catalytic cycle in the Suzuki reaction.

ligand dissociation to produce palladium(0) colloids or nanoparticles under these conditions. With these aspects in mind and in the quest for to investigate whether there is a difference in catalytic activity between all the Pd complexes **1**–**8**. Actually, as shown in Table 4, we observed a difference in catalytic activity. That is, Pd complexes **1**, **2**, **5**, and **6** exhibited higher catalytic activity than Pd complexes **3**, **4**, **7**, and **8** and also compared with the starting complexes $[PdCl_2(MeCN)_2]$ and $[PdCl_2(C_6H_5CN)_2]$. In the case of the complexes **1**, **2**, **5**, and **6**, TEM pictures clearly show the formation of Pd(0) nanoparticles, which is the true active species during the coupling reaction (Figs. 4 and 5 and See F-12, Supporting material). In all the reactions catalysed by the complexes **1**, **2**, **5**, and **6**, yellow and orange Pd(II) solution rapidly turns black at the end of reaction, which attributed to the formation of palladium(0) nanoparticles which serves as a source of the actual catalyst following oxidative addition of the activated or non-activated aryl halide substrate to a Pd atom on the surface of the nanoparticle. On the other hand, in the case of the complexes **3**, **4**, **7**, and **8**, TEM pictures clearly indicate with no formation of Pd(0) nanoparticles under the

Table 6
Results of the Suzuki–Miyaura cross-coupling reactions of aryl halides with phenylboronic acid using complex **1**–**8**.[a]

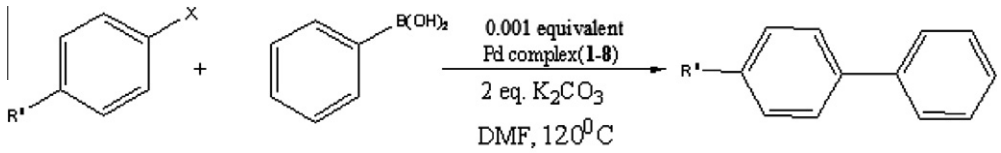

Entry	R^1	X	Yield (%)[c]/(TON)[d]							
			1	**2**	**3**	**4**	**5**	**6**	**7**	**8**
a	CH_3	I	99 (990)	99 (990)	50 (500)	55 (550)	94 (940)	98 (980)	45 (450)	50 (500)
b	CH_3	Br	99 (990)	95 (950)	58 (580)	54 (540)	97 (970)	96 (960)	48 (480)	54 (540)
c	CH_3	Cl	75 (750)	70 (700)	43 (430)	40 (400)	72 (720)	68 (680)	42 (420)	36 (360)
d	H	I	93 (930)	99 (990)	55 (550)	47 (470)	95 (950)	98 (980)	48 (480)	51 (510)
e	H	Br	97 (970)	99 (990)	43 (430)	49 (490)	98 (980)	99 (990)	45 (450)	47 (470)
F	H	Cl	60 (600)	56 (560)	26 (260)	20 (200)	50 (500)	58 (580)	27 (270)	29 (290)
g[b]	CH_3	Br	5	3	58	54	4	5	48	54

[a] All reactions were carried out using 2.0 mmol activated or non-activated, 2.0 mmol phenylboronic acid, 4.0 mmol K_2CO_3, 0.001 equivalent Pd complex and 10 ml DMF at 120 °C for 12 h.
[b] 300 Equivalent of Hg(0).
[c] Isolated yield.
[d] Mol(substrate) X% yield/mol(Pd).

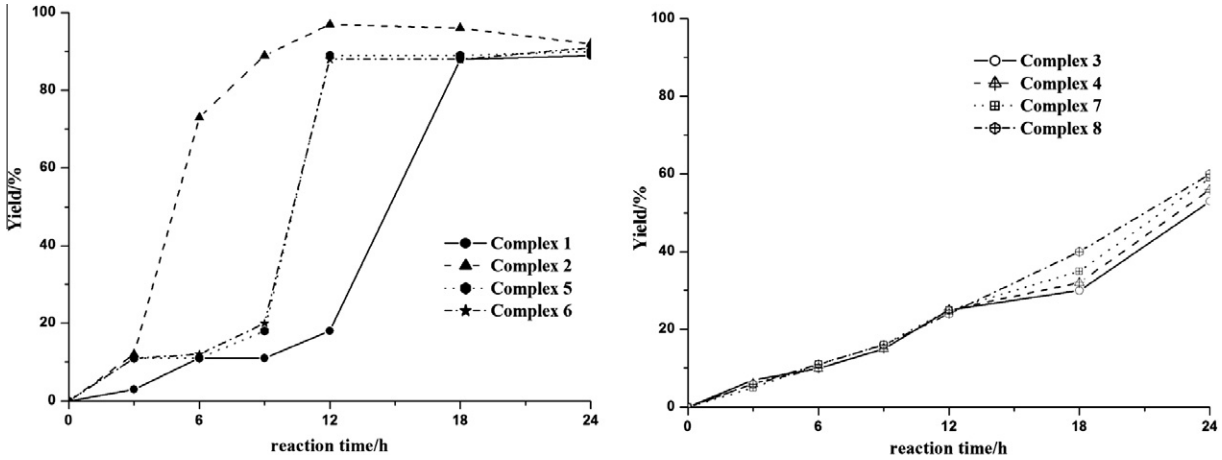

Fig. 7. Yield vs reaction time for Heck coupling of bromobenzene and *n*-butylacrylate using **1**–**8**.

same conditions (See F-13, Supporting material). This observation suggested that the ease of dissociation of the ligand promoted the formation of the Pd(0) nanoparticles occur more easily in complexes **1**, **2**, **5**, and **6** in comparison to the **3**, **4**, **7**, and **8** complexes. A high isolated yield to the Mizoroki–Heck coupling product was obtained for activated aryl iodides or bromides (Table 4, entry d, e, j and k) than activated aryl chlorides (Table 4, entry f and l) for **1**, **2**, **5**, and **6** complexes in comparison to **3**, **4**, **7**, and **8** complexes. Extending the reaction time up to 48 h did not give better results for activated aryl chlorides. However, for non-activated iodo or bromo or chlorobenzene, the desired coupled product yield was obtained in 48–92%, corresponding to TON of 480–920 in **1**, **2**, **5**, and **6** complexes as compared to 30–68% yield with TON of 300 to 680 in **3**, **4**, **7**, and **8** complexes (Table 4, entry a, b, c, g, h and i). The low yields obtained with aryl chloride or non-activated aryl chlorides are due to the stronger C_{sp2}—Cl bonds of aryl chlorides than those of the heavier congeners. Moreover, the observed catalytic activity of our pre-catalysts (**1**, **2**, **5**, and **6**) are better than already reported Pd–imidazole complexes in the literature [45–60]. It has been known that Hg(0) can poison the catalytic property of a metal(0) species by amalgamating the metal or absorbing on the metal surface in a heterogeneous catalysis [82,83]. In our study we also found that the addition of excess Hg(0) (Hg:Pd = 300:1) indeed totally deactivated the coupling reaction in **1**, **2**, **5**, and **6** complexes, while the addition of excess Hg(0) did not deactivated the coupling reaction in **3**, **4**, **7**, and **8** complexes (Table 5, entry a, b). This result might suggest that the actual catalytic species is Pd(0) species as reported [84]. We assume that the imidazole containing Pd(II) complexes might be reduced to a stable palladium(0) nanoparticles which in an active species for the catalytic cycle. The reason for the induction period of pre-catalyst**s 1**–**8** as shown in Fig. 7 is also not clear at present. However, we believe the difference in the rate of ligand dissociation to produce the real catalytic species causes the different induction periods between Pd pre-catalysts **1**–**8**. Further investigation of the true activation mechanism for imidazole containing Pd(II) complexes and its practical applications are undergoing in our laboratory.

*3.4.2. Suzuki–Miyaura coupling catalyzed by Pd complexes **1**–**8***

The Palladium–imidazole complexes (**1**–**8**) were tested as catalysts in the model Suzuki–Miyaura reaction of selected activated or non-activated aryl halides with phenylboronic acid (Table 6). Here as well, complexes **1**, **2**, **5**, and **6** exhibited higher catalytic activity than **3**, **4**, **7**, and **8** (Table 6) and also compared with the starting complexes $[PdCl_2(MeCN)_2]$ and $[PdCl_2(C_6H_5CN)_2]$; that is, the reaction of activated or non-activated aryl halides with phenylboronic acid in the presence of 0.001 equivalent of Pd complex (**1**, **2**, **5**, and **6**) in DMF at 120 °C for 12 h gave 50–99% yield to the Suzuki–Miyaura coupling product, corresponding to TON of 500–990, whereas use of Pd complex **3**, **4**, **7**, and **8** under the same conditions afforded the product in 20 to 58% yield with TON of 200–580. The results presented in Table 6 are in agreement with the earlier observation that imidazoles incorporating an N—H bond do not catalyze the coupling reaction [85,86]. However, neither of the imidazole complexes studied, **1**–**8**, obeyed this rule, affording 20–99% product yield. The higher catalytic activity of these complexes, which contains imidazole based ligands, had been shown better results in comparison to Hayashi et al. [74] and Trzeciak et al. [61]. To explain the reason behind the higher catalytic activity of **1**, **2**, **5**, and **6** complexes compared to **3**, **4**, **7**, and **8** is due to the easily dissociation of the ligand from the respective complex results into formation of Pd nanoparticles (Fig. 6) that activate substrates of the Suzuki–Miyaura reaction. We also carried out the Hg poisoning experiments. In our study, we found that the addition of excess Hg(0) (Hg:Pd = 300:1) indeed deactivated the reaction in **1**, **2**, **5**, and **6** complexes, although no activity has been diminished in complexes **3**, **4**, **7**, and **8** as shown in Table 6 (entry g).

4. Conclusion

In this work we have synthesized and characterized a series of new palladium(II) complexes with different imidazole derivatives. We also determined the structures in the solid state of the complexes dichlorobis(1-phenylimidazole)palladium(II) (**1**) and dibromobis(1-(4-Methoxyphenyl)-1*H*-imidazole)palladium(II) (**6**) using single-crystal X-ray diffractometry. The newly synthesized complexes were successfully used in the Mizoroki–Heck reaction and the Suzuki–Miyaura coupling reaction. While all eight of the complexes screened were found to be catalytically active, the best results were obtained for the complexes **1**, **2**, **5** and **6** in comparison to the complexes **3**, **4**, **7**, and **8**, which is due to ease of dissociation of the ligand lead to Pd nanoparticles that assist higher catalytic activity of these complexes. Further investigations towards other coupling reactions using our catalytic system and catalytic mechanism are currently in progress in our laboratory.

Acknowledgements

We gratefully acknowledge financial support from University Grants Commission, New Delhi (Grant No. F.4–2/2006(BSR)/13–76/2008(BSR)) and DST, New Delhi (SR/FT/CS-104/2011). We also thank Dr. S. Uma, and the Head, Department of Chemistry, University of Delhi and Professor D.S. Pandey, Department of Chemistry, Faculty of Science, Banaras Hindu University, Varanasi, India for

their kind encouragement. Special thanks are due to Professor P. Mathur, Department of Chemistry, Indian Institute of Technology, Mumbai and National Single Crystal X-ray Diffraction Facility, Indian Institute of Technology, Mumbai and The Director, USIC, University of Delhi for providing single crystal X-ray data and GC-MS facility from AIRF center of JNU, New Delhi. We acknowledge funding from the National Science Foundation (CHE0420497) for the purchase of the *APEX* II diffractometer.

Appendix A. Supplementary material

CCDC 784764 & 828055 (complex **1**) and 784765 (complex **6**) contain the supplementary crystallographic data for this paper. These data can be obtained free of charge from The Cambridge Crystallographic Data Centre via www.ccdc.cam.ac.uk/data_request/cif. Supplementary data associated with this article can be found, in the online version, at http://dx.doi.org/10.1016/j.ica.2012.08.003.

References

[1] J. Tsuji, Palladium Reagents and Catalysts, Wiley, New York, 2004. Chapter 3.
[2] F. Diederich, P.J. Stang, Metal-Catalyzed Cross-Coupling Reactions, VCH, Weinheim, 1997.
[3] M. Beller, Transition Metals for Organic Synthesis: Building Blocks and Fine Chemicals, VCH, Weinheim, 2004.
[4] A.M. Trzeciak, J.J. Ziółkowski, Coord. Chem. Rev. 251 (2007) 1281.
[5] U. Christmann, R. Vilar, Angew. Chem., Int. Ed. 44 (2005) 366.
[6] A.F. Littke, G.C. Fu, Angew. Chem., Int. Ed. 42 (2002) 4176.
[7] J.P. Wolfe, S.L. Buchwald, Angew. Chem., Int. Ed. 38 (1999) 2413.
[8] E.R. Strieter, D.G. Blackmond, S.L. Buchwald, J. Am. Chem. Soc. 125 (2003) 13978.
[9] D. O'Keefe, M. Dannock, S. Marcuccio, Tetrahedron Lett. 33 (1992) 6679.
[10] K.C. Kong, C.H. Cheng, J. Am. Chem. Soc. 113 (1991) 6313.
[11] W.A. Herrmann, C. Brossmer, K. Öfele, C.P. Reisinger, M. Beller, Angew. Chem., Int. Ed. 34 (1995) 1844.
[12] M. Beller, H. Fischer, W.A. Herrmann, K. Öfele, C. Brossmer, Angew. Chem., Int. Ed. 34 (1995) 1848.
[13] M. Beller, T.H. Riermeier, Eur. J. Inorg. Chem. (1998) 29.
[14] W.A. Herrmann, C. Brossmer, C.-P. Reisinger, T.H. Riermeier, K. Ögele, M. Beller, Chem. Eur. J. 3 (1997) 1357.
[15] E.A.B. Kantchev, J.Y. Ying, Organometallics 28 (2009) 289–299.
[16] M. Catellani, E. Motti, N. Della Cá, Acc. Chem. Res. 41 (2008) 1512–1522.
[17] R.B. Bedford, C.S.J. Cazin, M.B. Hursthouse, M.E. Light, V.J.M. Scordia, Dalton Trans. (2004) 3864.
[18] C. Barnard, Platinum Met. Rev. 53 (2009) 67.
[19] J. Dupont, M. Pfeffer, Palladacycles, Wiley-VCH, Weinheim, 2008.
[20] W.A. Herrmann, C.-P. Reisinger, M. Spiegler, J. Organomet. Chem. 557 (1998) 93.
[21] T. Weskamp, V.P. Böhm, W.A. Herrmann, J. Organomet. Chem. 585 (1999) 348.
[22] W.A. Herrmann, Angew. Chem., Int. Ed. 41 (2002) 1290.
[23] W.A. Herrmann, K. Öfele, D.V. Preysing, S.K. Schneider, J. Organomet. Chem. 687 (2003) 229.
[24] C.E. Ellul, G. Reed, M.F. Mahon, S.I. Pascu, M.K. Whittlesey, Organometallics 29 (2010) 4097.
[25] C.-C. Yang, P.-S. Lin, F.-C. Liu, I.J.B. Lin, Organometallics 29 (2010) 5959.
[26] C. Fliedel, P. Braunstein, Organometallics 29 (2010) 5614.
[27] H. Yang, X. Han, G. Li, Y. Wang, Green Chem. 11 (2009) 1184.
[28] A. Arnanz, C. González-Arellano, A. Juan, G. Villaverde, A. Corma, M. Iglesias, F. Sánchez, Chem. Commun. 46 (2010) 3001.
[29] S. Wittmann, A. Schätz, R.N. Grass, W.J. Stark, O. Reiser, Angew. Chem., Int. Ed. 49 (2010) 1867.
[30] K. Cavell, Dalton Trans. (2008) 6676.
[31] M. Poyatos, W. McNamara, C. Incarvito, E. Clot, E. Peris, R.H. Crabtree, Organometallics 27 (2008) 2128.
[32] F.E. Hahn, M.C. Jahnke, Angew. Chem., Int. Ed. 47 (2008) 3122.
[33] N. Marion, S.P. Nolan, Acc. Chem. Res. 41 (2008) 1440.
[34] W.-M. Dai, Y. Li, Y. Zhang, K.W. Lai, J. Wu, Tetrahedron Lett. 45 (2004) 1999.
[35] W.-M. Dai, K.K.Y. Yeung, J.-T. Liu, Y. Zhang, I.D. Williams, Org. Lett. 4 (2002) 1615.
[36] W.-M. Dai, K.K.Y. Yeung, Y. Wang, Tetrahedron 60 (2004) 4425.
[37] W.-M. Dai, Y. Zhang, Tetrahedron Lett. 46 (2005) 1377.
[38] J. Vĉelák, J. Storch, M. Czakóová, J. Čermák, J. Mol. Catal. A: Chem. 222 (2004) 121.
[39] C. Mazet, L.H. Gade, Eur. J. Inorg. Chem. (2003) 1161.
[40] M.T. Reetz, G. Lohmer, R. Schwickardi, Angew. Chem., Int. Ed. 37 (1998) 481.
[41] M. Beller, A. Zapf, Synlett 12 (1998) 792.
[42] M. Julia, M. Duteil, C. Grard, E. Kuntz, Bull. Soc. Chim. Fr. (1973) 2791.
[43] N.T.S. Phan, M.V.D. Sluys, C.W. Jones, Adv. Synth. Catal. 348 (2006) 609.
[44] A. Togni, L.M. Venanzi, Angew. Chem., Int. Ed. 33 (1994) 497.
[45] W. Cabri, I. Candiani, A. Bedeschi, R. Santi, J. Org. Chem. 58 (1993) 7421.
[46] R. van Asselt, C.J. Elsevier, Tetrahedron 50 (1994) 323.
[47] M.C. Done, T. Rüther, K.J. Cavell, M. Kilner, E.J. Peacock, N. Braussaud, B.W. Skelton, A.H. White, J. Organomet. Chem. 607 (2000) 78.
[48] T. Rüther, M.C. Done, K.J. Cavell, E.J. Peacock, B.W. Skelton, A.H. White, Organometallics 20 (2001) 5522.
[49] J. Silberg, T. Schareina, R. Kempe, K. Wurst, M.R. Buchmeiser, J. Organomet. Chem. 622 (2001) 6.
[50] T. Kawano, T. Shinomaru, I. Ueda, Org. Lett. 4 (2002) 2545.
[51] G.A. Grasa, R. Singh, E.D. Stevens, S.P. Nolan, J. Organomet. Chem. 687 (2003) 269.
[52] C. Nájera, J. Gil-Moltó, S. Karlström, L.R. Falvello, Org. Lett. 5 (2003) 1451.
[53] S. Iyer, G.M. Kulkarni, C. Ramesh, Tetrahedron 60 (2004) 2163.
[54] A.K. Gupta, C.H. Song, C.H. Oh, Tetrahedron Lett. 45 (2004) 4113.
[55] K.R. Reddy, G.G. Krishna, Tetrahedron Lett. 46 (2005) 661.
[56] X. Cui, Y. Zhou, N. Wang, L. Liu, Q.-X. Guo, Tetrahedron Lett. 48 (2007) 163.
[57] S. Haneda, Z. Gan, K. Eda, M. Hayashi, Organometallics 26 (2007) 6551.
[58] R.A. Gossage, H.A. Jenkins, P.N. Yadav, Tetrahedron Lett. 45 (2004) 7689.
[59] C.R. Eisnor, R.A. Gossage, P.N. Yadav, Tetrahedron 62 (2006) 3395.
[60] S. Haneda, C. Ueba, K. Eda, M. Hayashi, Adv. Synth. Catal. 349 (2007) 833.
[61] M.S. Szulmanowicz, W. Zawartka, A. Gniewek, A.M. Trzeciak, Inorg. Chim. Acta 363 (2010) 4346.
[62] T. Mizoroki, K. Mori, A. Ozaki, Bull. Chem. Soc. Jpn. 44 (1971). 581-581.
[63] R.F. Heck, J.P. Nolley, J. Org. Chem. 37 (1972) 2320.
[64] A. Suzuki, Pure Appl. Chem. 57 (1985) 1749.
[65] A. Suzuki, Pure Appl. Chem. 63 (1991) 419.
[66] A. Suzuki, Pure Appl. Chem. 66 (1994) 213.
[67] N. Miyaura, A. Suzuki, Chem. Rev. 95 (1995) 2457.
[68] M.S. Kharasch, R.C. Seyler, F.R. Mayo, J. Am. Chem. Soc. 60 (1938) 882.
[69] A. Hatzidimitriou, A. Gourdon, J. Devillers, J.-P. Launay, E. Mena, E. Amouyal, Inorg. Chem. 35 (1996) 2212.
[70] G.M. Sheldrick, Bruker Analytical X-ray Division, Madison, WI, 1998.
[71] G.M. Sheldrick, SHELX-97; Programme for Refinement of Crystal Structures, University of Gottingen, Gottingen, Germany, (1997).
[72] A.L. Platon, Acta Crystallogr., Sect. 46A (1990) C34.
[73] J.R. Ferraro, Low Frequency Vibrations of Inorganic and Coordination Compounds, Plenum Press, New York, 1971. 163.
[74] K. Kawamura, S. Haneda, Z. Gan, K. Eda, M. Hayashi, Organometallics 27 (2008) 3748.
[75] Y. Han, H.V. Huynh, L.L. Koh, J. Organomet. Chem. 692 (2007) 3606.
[76] A.J. Mota, A. Dedieu, P. Kuhn, D. Matt, R. Welter, M. Neuburger, Dalton Trans. (2005) 3155.
[77] R. Wang, J.-C. Xiao, B. Twamley, J.M. Shreeve, Org. Biomol. Chem. 5 (2007) 671.
[78] K. Kurdziel, S. Olejniczak, A. Okruszek, T. Głowiak, R. Kruszyński, S. Materazzi, M.J. Potrzebowski, J. Organomet. Chem. 691 (2006) 869.
[79] J. Vicente, A. Arcas, F. Juliá-Hernández, D. Bautista, P.G. Jones, Organometallics 29 (2010) 3066.
[80] G.R. Desiraju, T. Steiner, The Weak Hydrogen Bond in Structural Chemistry and Biology, Oxford University Press, Oxford, 1999.
[81] J.G. de Vries, Dalton Trans. (2006) 421.
[82] C. Adamo, C. Amatore, I. Ciofini, A. Jutand, H. Lakmini, J. Am. Chem. Soc. 128 (2006) 6829.
[83] S. Pal, W.S. Hwang, I.J.B. Lin, C.S. Lee, J. Mol. Catal. A: Chem. 269 (2007) 197.
[84] V.V. Grushin, H. Alper, Chem. Rev. 94 (1994) 1047.
[85] C.J. Mathews, P.J. Smith, T. Welton, J. Mol. Catal. A: Chem. 206 (2003) 77.
[86] I. Ozdemir, B. Centinkaya, S. Demir, J. Mol. Catal. A: Chem. 208 (2004) 109.